

# Phosphoregulatory protein 14-3-3 facilitates SAC1 transport from the endoplasmic reticulum

Kanika Bajaj Pahuja<sup>a,b,1,2</sup>, Jinzhi Wang<sup>c</sup>, Anastasia Blagoveshchenskaya<sup>c</sup>, Lillian Lim<sup>a</sup>, M. S. Madhusudhan<sup>d,e,f</sup>, Peter Mayinger<sup>c</sup>, and Randy Schekman<sup>a,b,1</sup>

<sup>a</sup>Department of Molecular and Cell Biology, University of California, Berkeley, CA 94720; <sup>b</sup>Howard Hughes Medical Institute, University of California, Berkeley, CA 94720; <sup>c</sup>Division of Nephrology & Hypertension, Oregon Health and Science University, Portland, OR 97239; <sup>d</sup>Department of Biology, Indian Institute of Science Education and Research, Pune 411008, India; <sup>e</sup>Bioinformatics Institute, Singapore 136781; and <sup>f</sup>Department of Biological Sciences, National University of Singapore, Singapore 117543

Contributed by Randy Schekman, May 13, 2015 (sent for review August 26, 2013; reviewed by Charles Barlowe)

Most secretory cargo proteins in eukaryotes are synthesized in the endoplasmic reticulum and actively exported in membrane-bound vesicles that are formed by the cytosolic coat protein complex II (COPII). COPII proteins are assisted by a variety of cargo-specific adaptor proteins required for the concentration and export of secretory proteins from the endoplasmic reticulum (ER). Adaptor proteins are key regulators of cargo export, and defects in their function may result in disease phenotypes in mammals. Here we report the role of 14-3-3 proteins as a cytosolic adaptor in mediating SAC1 transport in COPII-coated vesicles. Sac1 is a phosphatidylinositol-4 phosphate (PI4P) lipid phosphatase that undergoes serum dependent translocation between the endoplasmic reticulum and Golgi complex and controls cellular PI4P lipid levels. We developed a cell-free COPII vesicle budding reaction to examine SAC1 exit from the ER that requires COPII and at least one additional cytosolic factor, the 14-3-3 protein. Recombinant 14-3-3 protein stimulates the packaging of SAC1 into COPII vesicles and the sorting subunit of COPII, Sec24, interacts with 14-3-3. We identified a minimal sorting motif of SAC1 that is important for 14-3-3 binding and which controls SAC1 export from the ER. This LS motif is part of a 7-aa stretch, RLSNTSP, which is similar to the consensus 14-3-3 binding sequence. Homology models, based on the SAC1 structure from yeast, predict this region to be in the exposed exterior of the protein. Our data suggest a model in which the 14-3-3 protein mediates SAC1 traffic from the ER through direct interaction with a sorting signal and COPII.

SAC1 | 14-3-3 | COPII vesicles | reconstitution | adaptor protein

Most of the transmembrane secretory cargo proteins from the endoplasmic reticulum (ER) are selectively exported in cytosolic coat protein complex II (COPII) vesicles via direct interaction of their export motif with the COPII coat. The COPII coat core machinery consists of five cytosolic proteins: Sar1, Sec23, Sec24, Sec13, and Sec31 (secretory pathway proteins) (1). Sec24 is considered to be the primary subunit responsible for binding to membrane cargo proteins at the ER and concentrating them into the forming vesicle (2). Some of these cargo proteins require the assistance of cytosolic or membrane-spanning accessory adaptor proteins for their incorporation into COPII vesicles. Several adaptor proteins have been identified to assist the COPII machinery in yeast (3–5); however, fewer have been characterized in higher eukaryotes. In metazoans, ERGIC-53 mediates the export of blood clotting factors, Cathepsin Z and C and  $\alpha$ -1 antitrypsin (6), and SCAP [sterol-regulatory elementary binding protein (SREBP) cleavage activating protein] mediates the regulated transport of SREBP protein from the ER to the Golgi in cells that are sterol-deficient (7). Most COPII adaptor proteins are membrane-embedded, but at least one example of a cytosolic accessory protein, 14-3-3, has been proposed to control the anterograde trafficking of many of cell surface receptor proteins, possibly at the level of the ER (8). 14-3-3s are small

(30 kDa), acidic, and ubiquitously expressed eukaryotic proteins that are conserved from yeast to mammals and modulate various cellular processes by interacting with a variety of target proteins (9, 10). These include cell cycle regulation, signaling by MAP kinases, apoptosis, and transfer of signaling molecules between the nucleus and cytosol (11–14). Yeast cell viability depends on the expression of at least one of the two 14-3-3 isoforms (Bmh1 and Bmh2) (15). There are seven different isoforms in mammals ( $\beta$ ,  $\gamma$ ,  $\delta$ ,  $\epsilon$ ,  $\eta$ ,  $\sigma$ ,  $\theta$ ), some of which show differential tissue localization (14). Because of their redundant roles in cellular processes, depleting cellular levels of 14-3-3 to study a particular process poses a challenge. It is thought that their role in trafficking is to interfere with the ER retention/retrieval motif of target membrane proteins, and thus promote the transport of these cargos to the cell surface (16). For some proteins (e.g., KCNK3 and MHC class II, GPR15) (17–19), recruitment of 14-3-3 requires phosphorylation of a residue involved in 14-3-3 binding, whereas in other proteins (e.g., Kir6.2) 14-3-3 recognizes the correct assembly of multimeric proteins (20, 21).

In this paper we examine the role of 14-3-3 proteins as an adaptor for COPII vesicular transport of SAC1 (suppressor of actin mutations 1-like protein). SAC1 is a phosphatidylinositol-4 (PI4) lipid phosphatase that belongs to a family of enzymes with a CX<sub>5</sub>R(T/S) Sac catalytic domain, which is conserved from yeast to metazoans. Sac proteins control several cellular processes,

## Significance

Eukaryotes have evolved a multitrack transport process: the secretory pathway to route proteins to different destinations in a cell. Most cargo proteins originate on ribosomes bound to the endoplasmic reticulum (ER) and exit from the ER in membrane vesicles. The cytosolic coat protein complex II (COPII) coat is responsible for cargo protein sorting and vesicle budding from the ER. For some cargo proteins, additional cytosolic proteins serve to assist the core COPII machinery. One such cargo protein is the Sac1 lipid phosphatase, whose packaging into COPII vesicles depends upon the phosphopeptide binding protein, 14-3-3. Sac1 is essential to regulate cell signaling, division, and transport processes. We suggest that the 14-3-3 protein serves a regulatory role in the packaging of Sac1 into COPII vesicles.

Author contributions: K.B.P., P.M., and R.S. designed research; K.B.P., J.W., A.B., L.L., and M.S.M. performed research; K.B.P., J.W., and P.M. contributed new reagents/analytic tools; K.B.P. analyzed data; and K.B.P. and R.S. wrote the paper.

Reviewers included: C.B., Dartmouth Medical School.

The authors declare no conflict of interest.

<sup>1</sup>To whom correspondence may be addressed. Email: bajajk@gene.com or schekman@berkeley.edu.

<sup>2</sup>Present address: Department of Molecular Biology, Genentech Inc., South San Francisco, CA 94080.

This article contains supporting information online at [www.pnas.org/lookup/suppl/doi:10.1073/pnas.1509119112/-DCSupplemental](http://www.pnas.org/lookup/suppl/doi:10.1073/pnas.1509119112/-DCSupplemental).

including phosphoinositide homeostasis, membrane trafficking, and cytoskeleton organization. SAC1 is a 587-aa transmembrane protein with both N- and C-terminal domains exposed to the cytosol. Deletion of SAC1 in yeast and mammalian cells leads to changes in Golgi morphology and function and a SAC1 mouse knockout is embryonically lethal. Recently, SAC1 has been identified as *Drosophila* vesicle-associated protein binding partner and down-regulation of *Drosophila* vesicle-associated protein or SAC1 in *Drosophila* leads to the pathogenesis associated with amyotrophic lateral sclerosis (22).

It has been reported previously that SAC1 is localized to the Golgi membranes only when cells are starved for nutrients or growth factors, but remains in the ER under normal growth conditions (23, 24). Given the role for PI(4)P in vesicle traffic from the trans Golgi network, starvation conditions that lodge SAC1 and thus deplete the local supply of PI(4)P in the Golgi may suppress anterograde traffic in cells that must cease net cell growth. The regulation of SAC1 traffic may be crucial to the control of cell growth and anterograde membrane traffic.

The retrieval of mammalian SAC1 from the Golgi to the ER in the presence of growth factors or mitogens is controlled by COPI-mediated retrograde transport and requires the p38 MAPK pathway (23). Although the regulation of SAC1 retrieval from the Golgi has been reported, little is known about the control of SAC1 export from the ER under conditions of serum starvation. Recently, the N-terminal cytoplasmic domain of SAC1 was reported to contribute to Golgi localization in mammalian cells (25). We have established a cell-free reconstitution system that recapitulates the biogenesis and ER export of SAC1 and identified 14-3-3 proteins as an important factor in the packaging of SAC1 into COPII transport vesicles. Given the role of 14-3-3 proteins in various signaling pathways and the fact that SAC1 transport is affected by the p38 MAPK pathway, an understanding of the molecular role of 14-3-3 proteins in vesicular traffic could provide a mechanistic link between signaling and membrane assembly (23).

## Results

**SAC1 Packaging in COPII Vesicles Is Serum-Independent.** Based on predicted structural topology, SAC1 is a dual-pass transmembrane protein with the long N-terminal (~520 aa) and short C-terminal domains (20 aa), both exposed to the cytosol (Fig. 1A) (26). To examine the regulation of SAC1 export, we tagged mammalian SAC1 with a 3× HA epitope at its N terminus (cytosolic exposed) for expression in transfected COS7 cells. SAC1 localized to the *trans*-Golgi membrane, as determined by colocalization with Golgi marker Golgin-97, in a serum-deprived condition and localized to the ER in cells grown in the presence of serum (Fig. 1B). This localization pattern is similar to flag- and GFP-tagged versions of SAC1, as reported previously (23).

To establish a direct measure of the ER export of SAC1 and assess the role of COPII in trafficking of SAC1, we used an *in vitro* vesicle budding reaction supplemented with rat liver cytosol as a source of COPII proteins. A cell-free system was used to synthesize SAC1 in the presence of ER membranes from digitonin-permeabilized COS7 cells. This approach yielded two species that migrated at about ~65 kDa, as detected with anti-HA antibody and confirmed with anti-SAC1 antibody (Fig. 1C). Membranes with *in vitro* translated SAC1 were incubated in presence of rat liver cytosol and GTP and an ATP regenerating system. Vesicles formed at 30 °C were separated from the donor membranes by differential centrifugation and SAC1 was evaluated by SDS/PAGE and immunoblot. The lower band as detected by anti-HA antibody was sensitive to removal by a high salt wash (1M KOAc) of membranes and did not show energy and COPII dependence in its appearance in the budded vesicle fraction (Fig. 1C and Fig. S1). This species may represent a partially translated cytosolic domain of SAC1 that may associate

nonspecifically to membranes as reported earlier in case of yeast SAC1p with microsomal membranes (27). The upper band of

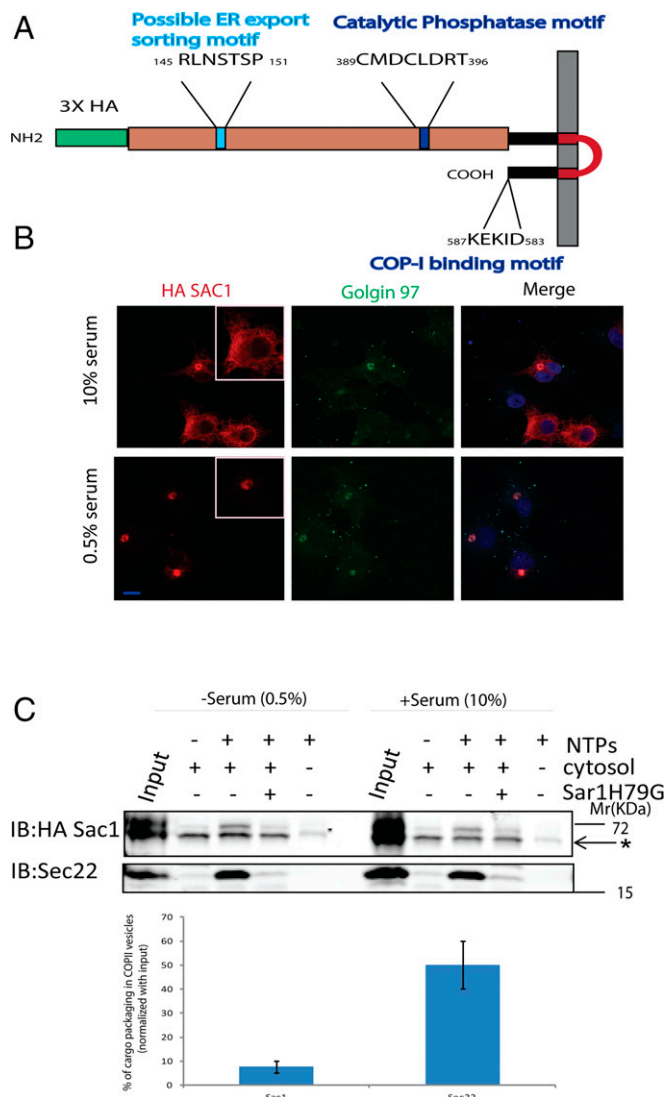


**Fig. 1. Packaging of SAC1 in COPII vesicles.** (A) Domain organization of mammalian SAC1 with 3xHA tag (green) at the N-terminal cytosolic domain (brown), RLNTSP motif (blue) examined in this study, and SAC1 catalytic motif (dark blue) two transmembrane segments (black) and C-terminal domain with COPI binding motif. (B) 3xHA-tagged SAC1 transported to the Golgi in serum-starved conditions in COS7 cells as observed by microscopy. COS7 cells were transfected with 3xHA-SAC1 and medium was changed to 10% serum and 0.5% serum and incubated for 24 h before fixing and staining for immunofluorescence microscopy with anti-HA antibody (red), anti-Golgin-97 (green), and DAPI (blue). SAC1 (red) displayed ER pattern in nonstarved cells (10% serum) and localized to the Golgi in starved cells (0.5% serum) as shown by colocalization (yellow) with Golgin-97 in merge images. Insets are shown on top in white box for enlarged single cell from the respective images. Magnification used was 63× on LSM710 confocal microscope. Insets are taken at 100× magnification. (C) SAC1 export in COPII vesicles was independent of serum starvation. HA-SAC1 buds equally efficiently from membranes prepared from starved and nonstarved cells (0.5% and 10% serum, respectively) in the presence of 4 mg/mL cytosol and energy in form of ATP, GTP. SAC1 budding was inhibited by addition of Sar1 dominant-negative mutant Sar1H79G. Sec 22 is an ER-Golgi cargo protein and served as a positive control for the budding reaction. Input was about 50% of the translated product used for the budding reaction. Packaging of SAC1 (top band-T and lower band-L), Sec22 was quantified using LICOR ODYSSEY analysis. Asterisk (\*) indicate lower band of HA-SAC1 after *in vitro* translation and probably partially translated SAC1.

HA-SAC1 (which will be referred to as SAC1) was incorporated efficiently in COPII vesicles in reactions containing cytosol at a concentration of 4 mg/mL and clearly showed energy dependence, as did a standard COPII cargo protein, Sec22 (Fig. 1C). HA-SAC1 budding was sensitive to the dominant-negative mutant of Sar1 (Sar1AH79G), a characteristic requirement for COPII-dependent transport (Fig. 1C). The budding efficiency of HA-SAC1 (9%) was comparable with the membranes from cells grown in the absence (0.5% serum) or presence (10% serum), as well as with the cytosol prepared from starved and nonstarved cells (Fig. 1C and Fig. S24). Moreover, HA-Sac1 transiently expressed in COS7 also showed comparable budding as in vitro translated Sac1 under both conditions (Fig. S1B). From this result we speculate that serum starvation may regulate SAC1 retrieval from the Golgi to the ER rather than its export from the ER (28).

**SAC1 RLSNTSP Motif Is Required for ER Export.** Mammalian SAC1 orthologs contain a dilysine COPI recognition motif, distinct from yeast Sac1p. Mutation of this motif results in SAC1 accumulation at the Golgi and a failure to be retrieved to the ER in cells stimulated with growth factor (23). Because COPI-mediated retrieval of SAC1 from the Golgi to the ER requires the p38 MAPK activity (23), we hypothesized that SAC1 phosphorylation/dephosphorylation controls its export/retrieval. We scanned the SAC1 sequence for putative p38 MAPK phosphorylation sites using GPS 2.1.1 (29). The sequence stretch RLSNTSP that spans region 145–151 in the N-terminal cytosolic domain resembled a potential 14-3-3 protein interaction site. Another predicted region from 508 to 513 was close to the transmembrane segment, and hence not considered. Because 14-3-3 proteins have been implicated in membrane trafficking, we tested the requirement of this motif in SAC1 transport with a deletion mutant (145–151  $\Delta$  mutant) and single-point Ala mutations of HA-SAC1 (R145A, L146A, S147A, N148A, T149A, S150A, P151A) (Fig. 2A). Deletion of this motif resulted in SAC1 retention in the ER, even in serum-starved cells (Fig. 2B), and showed no detectable packaging into COPII vesicles in vitro (Fig. 2C). As a control, the COPII cargo Sec22 was packaged normally in both incubations, suggesting that the trafficking defect was specific to SAC1. Ribophorin-I is an ER resident protein and is retained in the ER and not packaged into COPII vesicles. Single-point Ala mutations in this region did not result in measurable budding defects, suggesting that the 14-3-3 binding site involves multiple, possibly redundant interactions (Fig. S2). We evaluated double and triple Ala mutants in this region (Fig. 2A) and found that double mutations at L146 and S147 (LS/AA) and triple mutations at R145, L146, and S147 (RLS/AAA) resulted in a transport incompetent forms of SAC1 (Fig. 2C) that failed to localize to the ER-Golgi intermediate compartment with ERGIC-53 upon starvation (Fig. 2B). To summarize, we used SAC1 mutagenesis and vesicular budding assays to identify a minimal ER sorting motif (L146S147) for SAC1 export.

**SAC1 Mutant Is Enzymatically Active and LS Motif Is Exposed on Protein Surface.** To determine whether mutagenesis of SAC1 resulted in functional proteins, we measured the phosphatase activity of transport defective LS/AA SAC1 mutant protein. Flag-tagged versions of SAC1(WT), SAC1-LS/AA and phosphatase-deficient SAC1-C/S were expressed in COS7 cells and purified using M2-agarose beads. Aliquots of beads containing 0.4  $\mu$ g of immunopurified SAC1 protein were assayed for phosphatase activity using diocanoyl-PI(4)P as a substrate (30). Similar rates of change of absorbance that measured the free phosphate release upon PI(4)P hydrolysis was observed with SAC1(WT) and SAC1-LS/AA proteins (Fig. 3A). The results suggested that the catalytic activity of SAC1 is independent of its export from the ER and LS motif is not important for SAC1 phosphatase activity.

We modeled the LS motif in a 3D structural rendering of the N-terminal domain of the human protein based on the known structure of the yeast protein (Fig. 3B). The yeast and human homologs are 35% identical and at this level of sequence identity, it is expected that the models are sufficiently accurate to predict the overall scaffold and details of surface properties (31). The sequence from 145 to 151 (RLSNTSP) is predicted to be exposed to the surface and is therefore a potential interaction site. Furthermore, surface electrostatic analysis of the models show that this region of the protein is embedded in a negatively charged patch (Fig. 3C).

**SAC1 Binds 14-3-3 via RLSNTSP Motif.** Previous analysis of known 14-3-3 binding sites have defined two high-affinity phosphorylation-dependent binding motifs that are recognized by all 14-3-3

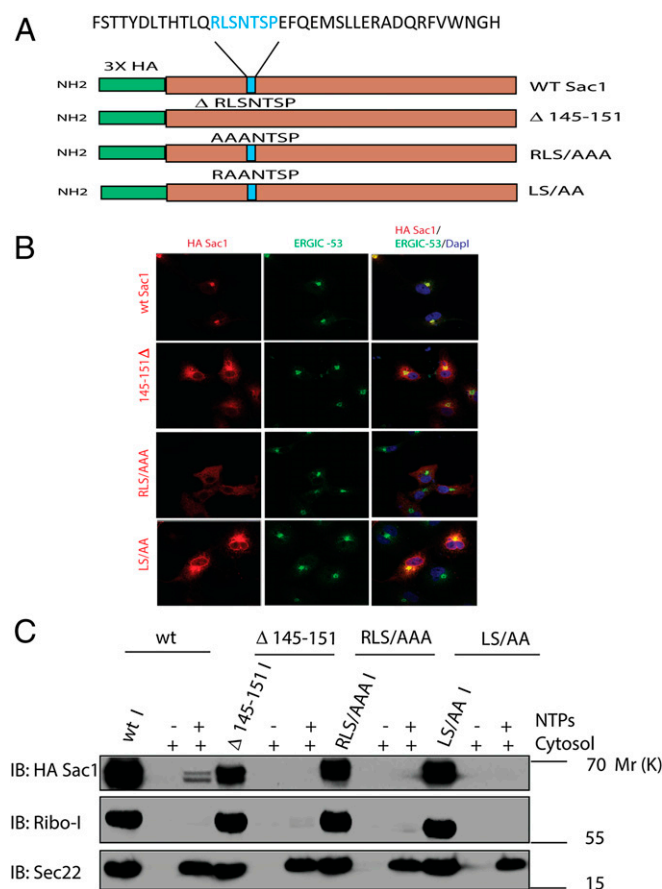


**Fig. 2.** RLSNTSP is the sorting motif for SAC1 ER export. (A) SAC1 mutant constructs used in the study and identification of 7-aa stretch similar to 14-3-3 binding site in the N-terminal cytoplasmic domain. (B) SAC1 mutants deleted in 7-aa stretch (145–151  $\Delta$ ), triple-alanine mutant (RLS/AAA), and double-alanine mutant (LS/AA) were retained in the ER under serum-starved conditions (0.5% serum) unlike SAC1(WT) and does not colocalize with ERGIC-53 that represents the ER–Golgi intermediate compartment. COS7 cells were transfected with HA-SAC1 and media was changed to 10% serum and 0.5% serum and incubated for 24 h before fixing and staining for immunofluorescence (red: HA-SAC1; green: ERGIC-53; blue: DAPI). Images were taken on LSM710 confocal and analyzed using LSM image browser. (Magnification: 63 $\times$ .) (C) SAC1 mutants ( $\Delta$ 145–151), triple alanine mutant (RLS/AAA), and double-alanine mutant (LS/AA) does not show COPII vesicular budding from the ER membranes assembled with in vitro translated SAC1. Sec22 as a COPII vesicular cargo control was budding efficiently from these membranes and membranes were not fragmented, as shown by the absence of ER membrane protein, Ribo-I. In vitro translated WT SAC1 shows nucleotide dependent COPII budding.



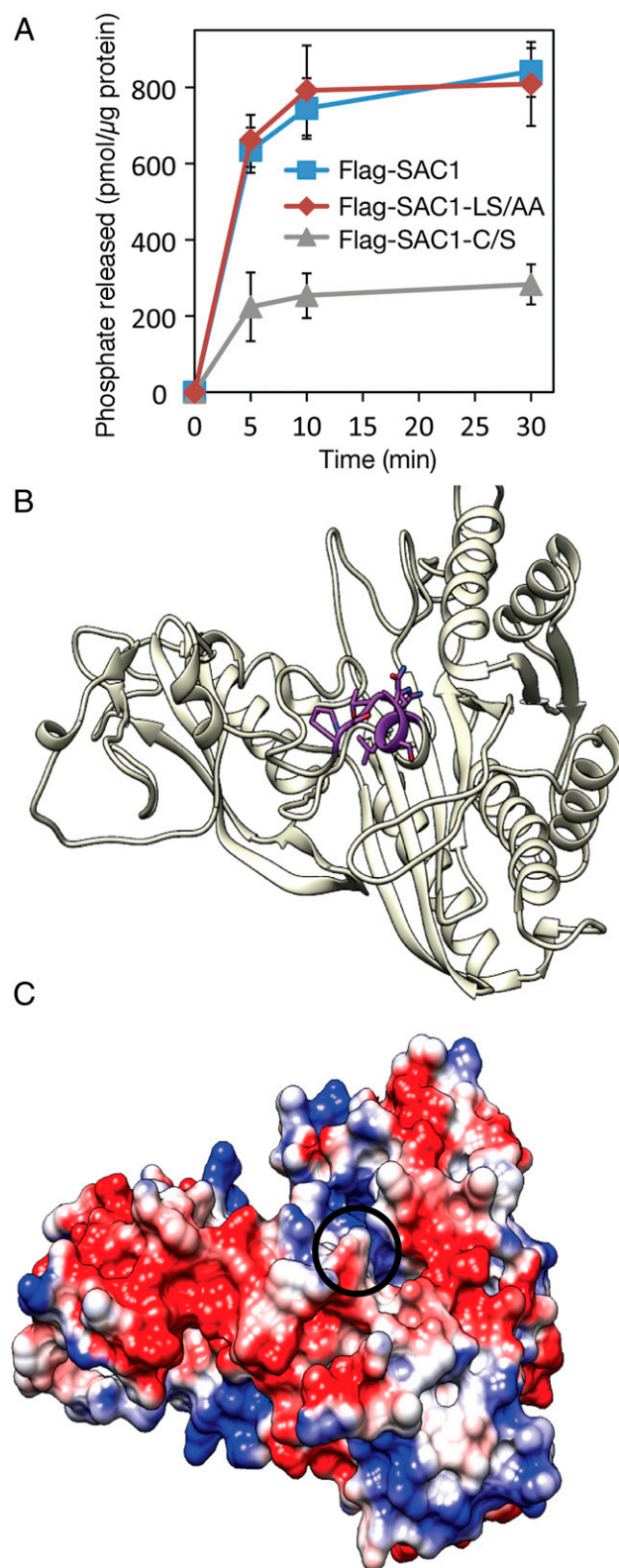


**Fig. 3.** The LS/AA SAC1 mutant is enzymatically active and the LS motif is exposed on the protein surface. (A) The LS/AA SAC1 mutant retains phosphatase activity. COS7 cells were transfected with plasmids for expressing flag-tagged versions of SAC1, SAC1-LS/AA, and phosphatase-deficient SAC1-C/S. Cells were lysed and flag-SAC1 proteins collected on M2-agarose beads. Aliquots of beads containing 0.4  $\mu$ g of immunopurified SAC1 protein were assayed for phosphatase activity using diocanoyl-PI(4)P as a substrate; release of phosphate from PI(4)P hydrolysis was followed at different time

isotypes: RSXpSXP (mode 1) and RXXXpSXP (mode 2), where pS represents phosphoserine (32, 33). However, different versions of phosphorylation-dependent sites that diverge significantly from these motifs have been described previously (34) and some 14-3-3 interactions are independent of phosphorylation. For example, binding of 14-3-3 to Kir 6.2, exoenzyme S, p190RhoGEF, and the R18 peptide inhibitor does not require a phosphorylated residue (21, 35–37). Because the RLSNTSP motif is similar to the 14-3-3 binding consensus motif, RXX(T/S)XP, we tested whether SAC1 interacts with 14-3-3 proteins. To address that, Hep3B cells or Hep3B cells stably expressing flag-SAC1 were transiently transfected with plasmids expressing HA-tagged 14-3-3 isoforms as indicated. The cells were lysed and flag-SAC1 was immunoprecipitated (IP) using anti-flag antibody and 14-3-3 was detected by co-IP using anti HA antibody. Under these conditions, SAC1 interacted with all 14-3-3 isoforms except 14-3-3  $\zeta$  (Fig. 4A). To further examine the functional correlation between 14-3-3 binding and SAC1 export, we performed GST pulldown analysis using GST tagged 14-3-3  $\beta$  and  $\epsilon$  proteins purified from *Escherichia coli*. Purified GST-14-3-3 and GST (control) were quantified and an equivalent amount of each was bound to glutathione-Sepharose beads for pulldown analysis using lysates of COS7 cells transfected with WT and mutant HA-SAC1 (Fig. 4B). SAC1(WT) showed specific interaction with both 14-3-3 isoforms and was pulled down efficiently with glutathione beads bound to 14-3-3 but not with control GST whereas mutations in the SAC1 RLSNTSP motif ( $\Delta$  145–151, LS/AA, and RLS/AAA) abolished 14-3-3 binding (Fig. 4B), consistent with the observation that these mutant proteins are retained in the ER and are defective in capture by COPII vesicles. None of the single-point Ala mutants in RLSNTSP motif affected binding to 14-3-3, consistent with their ability to sort into COPII vesicles (Fig. S3). Our data suggest that 14-3-3 binding to SAC1 via the RLSNTSP motif is necessary to mediate the efficient ER export of SAC1 and that L146 S147 is the minimal sorting motif within this sequence required for SAC1 transport. Moreover, SAC1 appears to be independent of phosphorylation but may require dimerization for efficient binding of 14-3-3 protein and transport, as reported earlier (23).

**14-3-3 Binds to Subunits of COPII Coat.** Although 14-3-3 proteins have no known enzymatic activity or particular subcellular localization, the protein may interact with COPII proteins in the cytoplasm, as suggested in a proteomic study of 14-3-3 interacting proteins (38). Capture of secretory membrane proteins in COPII vesicles is mediated by the Sec24 subunit of the Sec23/24 heterodimer, which interacts directly with the cytoplasmic face of the ER membrane. To probe the interaction of Sec24 and 14-3-3, we inserted Sec24 paralogs in pGADC1 and 14-3-3  $\theta$  in pGBDC1 in a yeast two-hybrid analysis.  $\beta$ -Galactosidase activity and growth on histidine-deficient selective medium revealed that 14-3-3  $\theta$  interacts with all Sec24 paralogs (A–D) (Fig. 4C and Fig. S4), although the interaction was not as strong as between Sec24A and Sec23A, which displayed growth on both histidine- and adenine-deficient plates. No interaction was observed between pGAD14-3-3  $\theta$  and pGBD Sec23A and controls. Based on the two-hybrid interaction results, we attempted to evaluate 14-3-3 as an adaptor bridge between SAC1 and Sec24 using a yeast three-hybrid interaction assay. However, human SAC1

points (5, 10, and 30 min). Data represent means  $\pm$  SD from two independent experiments. (B) RLSNTSP motif is exposed in human SAC1 model structure. Ribbon representation of N-terminal cytosolic domain of human SAC1 (residues 18–453) model structure with RLSNTSP motif highlighted in purple. (C) Surface electrostatic representation of SAC1 model calculated using APBS show RLSNTSP stretch (black circle) poses a negatively charge surface patch.

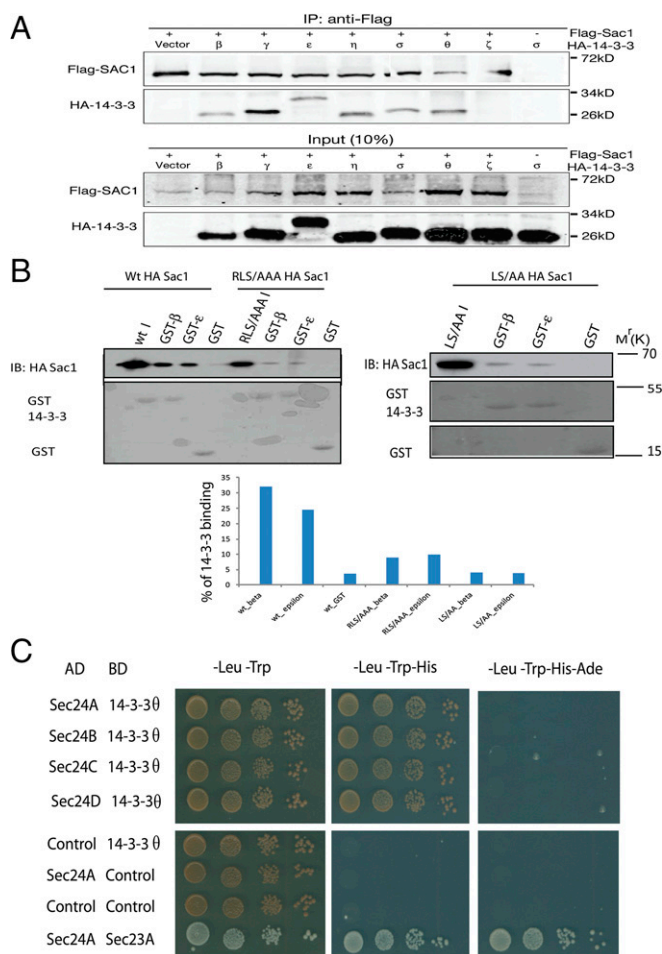


**Fig. 4.** 14-3-3 serves as an adaptor protein by binding SAC1 and Sec24. (A) SAC1 interacts with all isoforms of 14-3-3. Hep3B cells or Hep3B cells stably expressing flag-SAC1 were transiently transfected with plasmids for expressing HA-tagged 14-3-3 isoforms, as indicated. The cells were lysed and flag-SAC1 was immunoprecipitated (IP) using anti-flag M2 antibody. Proteins were separated by SDS/PAGE and analyzed by immunoblotting (using anti-flag M2 and anti-HA11 antibodies). (B) 14-3-3 interacts with HA-SAC1(WT) via RLSNTSP motif. GST-tagged 14-3-3 β and ε isoforms were purified from bacteria and bound to glutathione-Sepharose beads were used for pull downs. 14-3-3 β and ε proteins bound to glutathione-Sepharose beads were incubated with COS7 cells transfected with HA-SAC1(WT) and mutants. After incubation, the recovery of bound proteins was analyzed by immunoblot. 14-3-3 pulled down HA-SAC1(WT) expressed in COS 7 cells but did not interact with the Sac1 triple-Ala mutant (RLS/AAA) and double-Ala mutant (LS/AA). GST was used as a control for nonspecific binding. "I" refers to the 10% of the input lysate used for pull downs. GST-tagged 14-3-3 proteins and GST were detected on the blot using Ponceau staining. 14-3-3 binding to WT-Sac1 and mutant Sac1 was quantified using Adobe Photoshop Elements. (C) Yeast two-hybrid analyses indicated an interaction between 14-3-3 θ and Sec24s. Serial dilutions of the yeast colonies coexpressing the indicated constructs Sec24s in pGAD and 14-3-3 θ in pGBD were dotted on the indicated selective media (-Leu/-Trp, -Leu/-Trp-His, -Leu/-trp/-His/-Ade). Pictures were taken after 3 d of growth. Positive control reaction was between Sec23A and Sec24 and no growth was observed in selective media with empty control vectors.

constructs did not show interaction with 14-3-3 proteins and Sec24 and were not functional when expressed in yeast.

**SAC1 Budding Is Stimulated with Recombinant 14-3-3 Protein.** We examined whether packaging of SAC1 into transport vesicles depends on addition of 14-3-3 proteins in a budding reaction reconstituted with pure COPII proteins. The core cytosolic

components for a COPII vesicle budding reaction are Sar1, Sec23, Sec24, Sec13, and Sec31, which are sufficient to package a large number of membrane proteins in the yeast cell-free reaction (39). We observed that purified recombinant human COPII proteins were less efficient than crude rat liver cytosol in promoting SAC1 packaging with permeabilized COS7 cells, suggesting that an additional cytoplasmic factors may be involved in the sorting or budding process (Fig. 5A). Moreover, SAC1 budding was not preferentially dependent on one of the four Sec24 paralogs and displayed similar packaging with each Sec24 in reactions supplemented with 1 mg/mL cytosol, a concentration that by itself does not support incorporation of Sac1 into vesicles (Fig. 5A). This concentration of cytosol does support budding (as evidenced by Sec22 packaging) but not maximal incorporation of Sac1. To further analyze the role of 14-3-3 as a cytoplasmic factor required for SAC1 export, we purified an N-terminally GST-tagged 14-3-3 θ isoform from baculovirus-infected Sf9 insect cells (Fig. S5). The GST tag was cleaved from 14-3-3 and

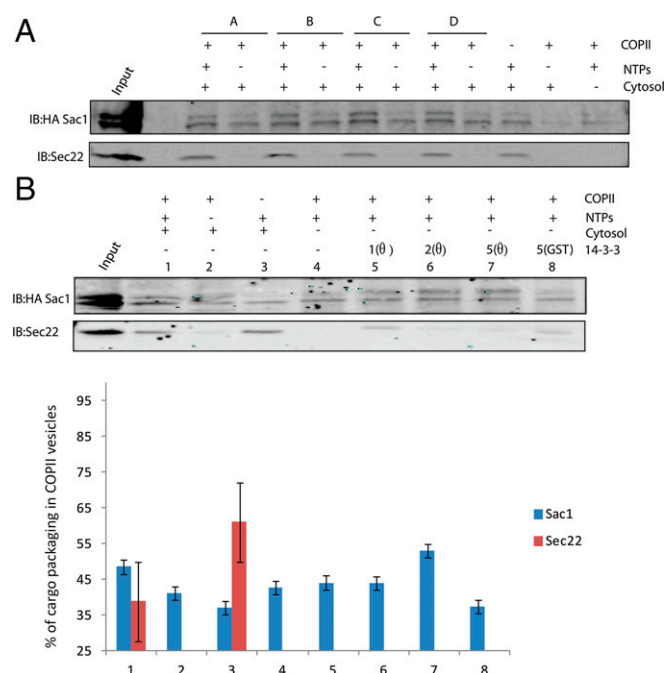


**Fig. 5.** SAC1 budding is sensitive to 14-3-3 interaction. (A) In vitro vesicular packaging of SAC1 was induced upon supplementing the reaction with purified COPII proteins, Sar1A, Sec23A/24(A/B/C/D), and Sec13/31, including cytosol (1 mg/mL), but did not show paralog specificity. A, B, C, and D indicate Sec24 paralogs. Alternate lanes indicate reactions in presence and absence of nucleotides. Sec22, the COPII vesicular marker, also showed enhanced in budding with COPII proteins. Input was 50% of the membranes used for reactions after in vitro translation. Sar1A, Sec23A/Sec24C, and Sec13/31 without cytosol showed minimal SAC1 budding with COS7 membranes. (B) SAC1 vesicular budding reaction was stimulated by the 14-3-3 θ isoform. HA-SAC1(WT) signal was further enhanced in isolated vesicle fraction when purified 14-3-3 θ protein was supplemented in the COPII budding reaction (reactions 5, 6, and 7) compared with the vesicle fraction from reaction 4, which was incubated with purified COPII proteins. Reaction 1 displays the vesicle fraction from a reaction performed with COPII proteins and 2 mg/mL cytosol. COPII includes Sar1A, Sec23A/24C, and Sec13/31 each added to 1-μM concentration. 14-3-3 θ concentrations used were 1 μM, 2 μM, 5 μM, and GST concentration was 5 μM. Input was 50% of membranes used for budding reaction. Sec22 packaging, used as a standard COPII marker, was not stimulated by addition of 14-3-3 proteins. Quantification of the data was done from two independent analysis (B and Fig. S6) using Odyssey (LICOR) and shown below as a fraction of HA-SAC1 and Sec22 budded in vesicles normalized with respect to input signal.



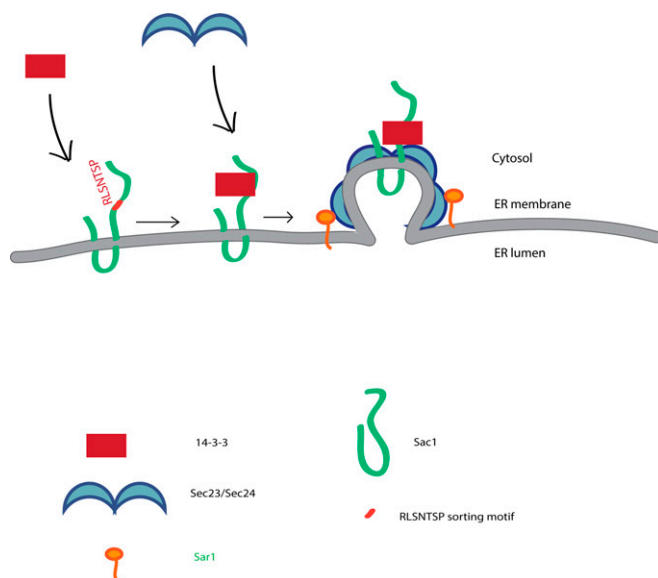


**Fig. 6.** Proposed model for 14-3-3 as adaptor protein for SAC1 budding. 14-3-3 binds N-terminal cytosolic domain of SAC1 via RLSNTSP motif and 14-3-3 protein recruit inner COPII coat proteins, Sec23/24, to form a quaternary complex and leads to concentration of SAC1 at ER exit site, the locus of COPII vesicle budding. 14-3-3 serves as a bridging protein that mediates the interaction between SAC1 and the COPII sorting subunit, Sec24.

purified protein at a range of concentrations (1–5  $\mu$ M) was used for in vitro COPII budding assays. The efficiency of HA-SAC1 budding was compared with another membrane cargo protein, Sec22, in reactions supplemented with the purified COPII proteins (Sar1B, Sec23A/24C, Sec13/31) and recombinant 14-3-3  $\theta$  protein. SAC1 packaging with COPII proteins was specifically stimulated by 14-3-3  $\theta$  protein (Fig. 5B, reactions 5, 6, and 7) but not control GST (Fig. 5B, reaction 8), and was comparable to the budding efficiency with COPII and cytosol (Fig. 5B, reaction 1). Sec22 packaging was unaffected by 14-3-3 and could not be reconstituted by the combination of 14-3-3 and COPII proteins (Fig. 5B), indicating that 14-3-3 selectively enhances the incorporation of SAC1 in COPII vesicles. These results confirmed that 14-3-3 proteins facilitate export of SAC1 in COPII vesicles and provided a novel mechanism of the action of 14-3-3 proteins in membrane trafficking.

## Discussion

Few examples of metabolic regulation of anterograde protein trafficking in metazoans are understood at a molecular mechanistic level. In mammalian cells, SREBP and an escort protein, SCAP, are transported from the ER to the Golgi membrane when the level of free cholesterol declines (7). The phosphoinositide phosphatase SAC1 also traverses this limb of the secretory pathway, regulated by growth factor and serum. In mammalian systems, the stress-activated MAPK p38 appears to play a critical role in transmitting nutrient signals for SAC1 retranslocation from the Golgi to the ER. All mammalian orthologs of SAC1 possess a C-terminal dilysine ER retention motif that interacts with COPI and is responsible for retrieval of SAC1 from the Golgi to the ER membranes in the presence of growth factors. In contrast, *Saccharomyces cerevisiae* SAC1 lacks a typical ER retrieval motif and employs Rer1p as an adaptor protein that impairs the interaction between SAC1p and Dpm1p and facilitates ER exit of Sac1 under glucose-deprived conditions (27).

In this study, we have established the molecular requirements for SAC1 export from the ER in mammalian cells and identified a role for 14-3-3 protein interaction with a putative sorting signal

on SAC1. SAC1 packaging in vesicles showed COPII dependence (inhibited by a Sar1 dominant-negative mutant), but was exported with comparable efficiencies in COPII vesicles from both starved and nonstarved cells. Despite this, HA-SAC1 displayed serum-dependent traffic between the ER and Golgi in cells as observed by immunofluorescence microscopy. Thus, we propose that SAC1 transport is regulated by growth factors at the level of retrieval from the Golgi.

We identified SAC1 mutants defective in transport to the Golgi in starved cells using cellular localization and *in vitro* reconstitution assays. The putative sorting motif (RLSNTSP) is localized to the N-terminal domain of SAC1. Homology-based modeling of the human SAC1 cytosolic domain (1–520) based on the yeast SAC1 structure indicates that this motif is exposed to solvent in a negatively charged surface patch. Mutations in this motif (LS/AA) do not interfere with SAC1 phosphatase activity, thus it is unlikely that the sorting mutations interfere with SAC1 protein folding. Our GST pulldown analysis demonstrates that this motif is required for SAC1 interaction with 14-3-3 proteins; moreover, the severity of reduced binding to 14-3-3 correlates with diminished SAC1 export from the ER *in vivo* and *in vitro*. SAC1 interacts with all 14-3-3 isoforms except 14-3-3  $\zeta$ , as revealed by co-IP analysis.

This work demonstrated that 14-3-3 is involved in anterograde traffic and not, as seen elsewhere, in blocking the retrieval of cargo and established a direct binding of 14-3-3 protein to a cargo molecule as a means of promoting transport. Most of the multimeric membrane proteins reported in literature that show 14-3-3-dependent trafficking have 14-3-3 and COPI protein binding motifs overlapping or in sufficiently close proximity to result in mutually exclusive interaction. Therefore, binding of 14-3-3 blocks the ER retrieval signal, facilitating the forward transport of their cognate cargoes. The SAC1 14-3-3 binding site (145–151) and COPI binding motif are in distinct cytosolic domains and mutations in 14-3-3 binding motif result in defects in ER export, which is inconsistent with the possibility that 14-3-3 proteins regulate forward transport by masking the ER retention signal.

14-3-3 proteins are known to form a complex with COPII coat proteins and have been implicated in the ER export of N-cadherin. We suggest that 14-3-3 serves as an adaptor protein for transport of SAC1 and other client proteins by interacting with the COPII sorting subunit, Sec24. Yeast-two hybrid analysis demonstrated an interaction between Sec24 paralogs (A, B, C, and D) and 14-3-3. Moreover, purified 14-3-3 protein stimulated the packaging of SAC1 in a vesicle budding reaction reconstituted with pure recombinant COPII proteins and membranes from COS7 cells to levels achieved with crude rat liver cytosol and COS7 membranes. Thus, 14-3-3 may be the only additional soluble adaptor protein required for COPII-mediated packaging of SAC1. Our results suggest a model where 14-3-3 proteins serve as a bridge between SAC1 and Sec24, possibly through a conformational change in SAC1, resulting in cargo concentration at the ER exit site (Fig. 6).

Further structural studies are required to understand the mechanism of ternary interaction between 14-3-3, SAC1, and Sec24 to classify 14-3-3 proteins as a bona fide COPII accessory protein. An interesting question is whether 14-3-3 proteins remain associated with SAC1 en route to the Golgi and help in regulating COPI binding and ER retrieval.

## Materials and Methods

**Plasmids, Peptides, and Antibodies.** To generate flag-tagged SAC1, the coding region of SAC1 was amplified by PCR using pEGFP-C1-SAC1 (40) as a template, digested with BamHI and SalI and subcloned into pCMV-3Tag-1A. The resulting pCMV-3Tag-1A-SAC1 plasmid expresses a version of SAC1 containing three N-terminal flag-epitopes in tandem. To generate HA-tagged SAC1, the SAC1 coding region was amplified from pcDNA3-flag-SAC1 (40) and subcloned into the pCS2-3x HA-tag vector between the FseI and AscI

sites for *in vitro* translation and vesicular budding assays. SAC1 mutants were generated by Quik-change site-directed mutagenesis. 14-3-3 (all seven isoforms) constructs in pCDNA3 vector were provided as generous gift from Blanche Schwappach (Göttingen University Medical School, Göttingen, Germany). 14-3-3 was subcloned from pCDNA3-14-3-3 into pGEX-4T vector for bacterial purification and pFAST-Bac-GST for baculovirus preparation. COPII baculoviruses generated from pFAST-Bac were generated in this laboratory. Sec24 (A, B, C, and D) were subcloned in pGADC1 vector and tau 14-3-3 was subcloned in pGBDC1 for yeast two-hybrid analysis. pCDNA3-myc-14-3-3  $\sigma$  was a gift from Gary Thomas (University of Pittsburgh, Pittsburgh, PA). Plasmids encoding mouse HA-tagged 14-3-3 isoforms were provided by Vivek Bhalla (Stanford University, Stanford, CA). Antibodies used in the study were: rabbit anti-HA antibody from Cell Signaling (catalog no. C29F4), Mouse anti-HA antibody from Covance (catalog no. 16B12), anti-ERGIC-53, anti-APP, anti-Sec22, anti-ribophorin I are rabbit antiserum, as described previously (41). Anti-flag M2 mouse monoclonal antibodies were purchased from Sigma (catalog no. F1804). Mouse 12CA5 monoclonal anti-HA11 antiserum was purchased from Abcam (catalog no. ab16918). Anti-flag M2-agarose was obtained from Sigma.

**Cell Culture.** COS7 cells and HeLa cells were cultured in DMEM (Sigma) supplemented with 10% FBS (Sigma) as indicated in newborn calf serum (NCS) and grown at 37 °C incubator at 5% CO<sub>2</sub>. Hep3B cells (ATCC no. HB-8064) were cultured in the Minimum essential medium (Eagle) supplemented with 2 mM L-glutamine and Earle's Balanced Salt Solution (EBSS) adjusted to contain 1.5 g/L sodium bicarbonate, 0.1 mM nonessential amino acids, and 1.0 mM sodium pyruvate, and 10% (vol/vol) FBS. To establish a cell line for stable expression of flag-SAC1, we transfected Hep3B cells with pCMV3Tag-1A-SAC1 (1  $\mu$ g of DNA mixed with 3  $\mu$ L lipofectamine2000). After 72 h, transfected cells were selected using 400  $\mu$ g/mL G418 (Geneticin). Established clones were screened by SDS/PAGE and subsequent immunoblot analysis using anti-flag M2 antibodies. For immunoprecipitations, Hep3B/Flag-SAC1 were plated in 10-cm dishes and grown to 80–90% confluence. Cells were transfected using various pMD-HA-14-3-3 vectors for expressing the individual isoforms (2.5  $\mu$ g each). A ratio of Lipofectamine 2000 to DNA of 4:3 was used in all transfection experiments. After 1-h incubation, the transfection mixture was replaced with normal culture medium (DMEM plus 10% FBS) and cells were allowed to grow for another 48 h.

**Immunofluorescence.** COS7 cells were transfected with HA-tagged versions of SAC1 and mutants by Lipofectamine 2000 using the manufacturer's protocol. COS7 cells were cultured on 25-mm glass coverslips, grown for 1 d, and transfected the next day with HA-SAC1 and mutants using Lipofectamine 2000. Medium was changed to 10% (vol/vol) NCS or 0.5% NCS on the third day and incubated in respective media for 24 h. Cells were fixed on fourth day with 3% paraformaldehyde for 30 min and permeabilized with 0.1% triton for 15 min at room temperature, followed by blocking with 1% BSA for 30 min. Primary antibodies were rabbit anti-HA (diluted 1:200) and mouse anti-Golgin-97 (diluted 1:200). Secondary antibodies were Alexa Fluor-488 goat anti-mouse IgG, and Alexa fluor-546 goat anti-rabbit IgG (diluted 1:100, Molecular Probes/Invitrogen). After staining cells with appropriate primary and secondary antibodies, coverslips were fixed on slides using mounting reagent containing DAPI. Images were visualized with a Zeiss Axio Observer Z1 fluorescent microscope and LSM 710 confocal microscope and captured with Metamorph software (Molecular Devices) and Zen10, respectively. Merges of images were performed with ImageJ and LSM Image Browser.

**Immunoprecipitation and Immunoblotting.** After transfection (48 h), cells were washed twice with ice-cold PBS and lysed on ice in immunoprecipitation NET-T buffer (150 mM NaCl, 5 mM EDTA, 10 mM Tris, pH 7.4, 1% Triton X-100) supplemented with Complete Protease Inhibitor Mixture (Roche Diagnostic). Cell lysates were centrifuged at 13,000  $\times$  g for 30 min to remove cell debris and the supernatants were precleared with Protein A-agarose (Zymed) for 1 h at 4 °C. Flag-tagged SAC1 was immunoprecipitated from the cell extracts using anti-flag M2-agarose overnight at 4 °C. The M2-agarose beads were washed four times with NET-T buffer. All of the samples were heated in boiling water in SDS sample buffer for 5 min and resolved by 12% SDS/PAGE. Proteins were transferred to nitrocellulose or PVDF (polyvinylidene difluoride) membranes, and immuno-detected using mouse monoclonal anti-HA11 (1:1,000) and M2 anti-flag (1:1,000) antibodies.

**SAC1 Phosphatase Assay.** COS7 cells were transfected by electroporation to express flag-tagged versions of SAC1, SAC1-LS/AA, or phosphatase-deficient SAC1-C/S (40). Two days after transfection, cells were washed once with PBS and harvested in mRIPA buffer [1% Nonidet P-40; 1% sodium deoxycholate; 150 mM

NaCl; 50 mM Tris-HCl, pH 8.0; protease inhibitors (Roche)]. Following centrifugation at 13,000  $\times$  g for 15 min, flag-tagged SAC1 protein was collected on M2-agarose beads. Pellets were washed twice in mRIPA containing 0.5 M NaCl and once in TBS at 4 °C. The assay was a modified version of the protocol described in ref. 30. Reaction buffer (50  $\mu$ L of 100 mM sodium acetate; 50 mM Bis-Tris; 50 mM Tris, pH 6.0, 0.002% porcine gelatin and 4 mM DTT), 50  $\mu$ M dioctanoyl-PI(4)P (Echelon Biosciences), and 0.4  $\mu$ g of recombinant SAC1 protein bound to M2-agarose was incubated at 37 °C. Reactions were stopped at various times by addition of 50  $\mu$ L of 100 mM NEM and the reaction mixture was centrifuged at 13,000  $\times$  g for 3 min. Supernatants (25  $\mu$ L) were pipetted into 96-well plates. Malachite Green solution (50  $\mu$ L: 1 volume 4.2% ammonium molybdate in 4 M HCl, 3 volumes of 0.045% Malachite Green, and 0.01% Tween 20) was added to each well. After incubation for 20 min at room temperature the OD<sub>620</sub> was measured.

**GST Pulldown Assay.** GST 14-3-3  $\beta$  and  $\epsilon$  isoforms were expressed and purified from BL-21DE3 codon plus using glutathione-Sepharose beads. Briefly, 14-3-3 cloned in pGEX4T was transformed in BL-21DE3 codon plus and was grown to OD<sub>600</sub> of 0.5 at 37 °C before induction with 0.1 mM isopropyl-1-thio- $\beta$ -D-galactopyranoside for 8 h at 25 °C. Cells were harvested the next day, suspended in TBST (50 mM Tris, 150 mM NaCl, 0.1% Tween, pH 7.4), and lysed using sonication in presence of 1% triton at 4 °C four times, 30 s each. Supernatants were collected after centrifugation at 14,000  $\times$  g for 30 min in SS34 rotor (Beckman) and incubated with glutathione 4-Sepharose (1 mL/L culture) and washed three times in TBST buffer for 3 h at 4 °C in a rotator. Beads were centrifuged at 3,000  $\times$  g for 3 min and washed four times with TBST to remove unbound and contaminant proteins; proteins were eluted using freshly prepared 10 mM glutathione in TBS buffer. Equivalent amounts of GST and GST-14-3-3 (15  $\mu$ g) were bound to glutathione-Sepharose beads (200  $\mu$ L) in PBS buffer for 2 h at 4 °C. Beads were centrifuged at 3,000  $\times$  g for 5 min, suspended in PBS + 0.1% BSA and incubated with lysates from COS7 cells transfected with WT SAC1 and mutant SAC1 for 2 h at 4 °C in a rotator. Beads were centrifuged and washed three times with PBS buffer to remove any nonspecific contaminants, GST-14-3-3 bound proteins were eluted in SDS loading dye and resolved on SDS/PAGE followed by immunoblot transfer. The PVDF blot was stained with Ponceau S stain to detect GST proteins and then washed for immunoblotting to detect HA-SAC1.

**Cytosol Preparation and COPII Protein Purification.** Rat liver cytosol was prepared as described previously (42) in Buffer E. Human Sar1A and Sar1B proteins were overexpressed in *E. coli* and purified as cleaved GST-fusions, as described for hamster Sar1 purifications (42). Sec13-31 and all paralogs of His-Sec24 (A, B, C, and D) were purified in complex with Sec23 using immobilized metal affinity chromatography from lysates of baculovirus-infected insect cells, as described previously (42, 43).

**In Vitro Transcription and Translation of 3XHA-SAC1.** Procedures for making cell-free mRNA, permeabilized cells, and subsequent *in vitro* translation were described previously (44), with some modifications. 3XHA-SAC1 was cloned into pCS2 vector and was used for *in vitro* transcription using a Promega *in vitro* transcription system (Promega) and a SAC1 construct cut with *Ascl* restriction enzyme. SAC1 was synthesized *in vitro* and assembled in presence of permeabilized COS7 membranes. The vesicle formation reaction and vesicle purification procedure is described as follows. In detail, COS7 cells grown in 3  $\times$  100-mm plates were washed in PBS, removed from plates with trypsin, and suspended in KHM buffer [110 mM KOAc, 20 mM Hepes, pH 7.2, 2 mM Mg(OAc)<sub>2</sub>] containing 10  $\mu$ g/mL<sup>-1</sup> soybean trypsin inhibitor. Cells were permeabilized with 40  $\mu$ g/mL<sup>-1</sup> digitonin for 5 min in ice-cold KHM and washed and resuspended in 100  $\mu$ L KHM. Endogenous RNA was degraded after addition of 1 mM CaCl<sub>2</sub> and 10  $\mu$ g/mL<sup>-1</sup> micrococcal nuclease and incubated at room temperature for 12 min. After incubation, the nuclease reaction was stopped by addition of 4 mM EGTA, and cells were sedimented and washed. Permeabilized RNA-free cells were resuspended in KHM buffer such that the measurement of absorbance (600 nm) for 5  $\mu$ L of cells in 500  $\mu$ L KHM was 0.1. These cells were added to an *in vitro* translation reaction with rabbit reticulocyte lysate (Promega) and RNA encoding HA-SAC1, and then incubated for 60 min at 30 °C. Donor membranes were washed three times with KHM buffer (unless indicated with KHM+1MKoAc) to remove non-translocated protein products and membrane bound peripheral proteins and resuspended in KHM buffer.

To form vesicles, we combined donor membranes with newly synthesized HA-SAC1, where indicated, with 4 mg/mL rat liver cytosol for cytosolic reaction or recombinant COPII proteins (adjusted to final concentration of 1  $\mu$ M each, supplemented with 1 mg/mL cytosol, an ATP regenerating system (40 mM creatine phosphate, 0.2 mg/mL<sup>-1</sup> creatine phosphokinase and 1 mM

ATP), 0.2 mM GTP followed by incubation at 30 °C for 1 h. Purified 14-3-3  $\theta$  protein at a final concentration of 1–5  $\mu$ M purified from insect cells was added to the budding reactions to supplement SAC1 packaging where indicated. Newly formed vesicles were separated from the more rapidly sedimenting donor membranes by centrifugation at 13,000  $\times$  g for 12 min. Vesicles were collected by centrifugation at 100,000  $\times$  g for 25 min in a TLA100 rotor and Optima TL ultracentrifuge. Vesicle pellets were resuspended and washed in 100  $\mu$ L cold KHM, centrifuged again, and finally solubilized in 20  $\mu$ L of 1% SDS and SDS loading dye. Vesicle fractions and original donor membranes were resolved on SDS-PAGE, transferred onto PVDF membranes and subjected to immunoblotting to detect HA-SAC1 and the positive control endogenous cargo proteins, amyloid precursor protein, ERGIC-53, and Sec22 using secondary fluorescent antibodies and the LICOR odyssey system.

**Yeast Two-Hybrid Interaction.** The yeast two-hybrid assay was carried out as described previously (45). *S. cerevisiae* strain pJ469 was used, and plasmid DNA transformations into the yeast strain were done using the LiAc method. Cells were cotransformed with human Sec24 cloned in pGAD and 14-3-3  $\theta$  cloned in pGBD plasmids and grown on agar plates containing complete medium lacking leucine and tryptophan for 2–3 d, to select for positive clones. Clones were then picked up from these plates and streaked on -leu/-trp plates, and allowed to grow for 1–2 d. These clones were then grown in complete media lacking leucine and tryptophan at 30 °C overnight, and equivalent amount of cells were spotted in serial dilution on selective medium -leu/-trp, -leu/-trp/-his, and -leu/-trp/-his/-ade plates, incubated at 30 °C

for 3–4 d. Images were captured and analyzed for interaction after 3 d of growth on the selective media.

**SAC1 Homology Modeling.** The 3D structure of human Sac 1 was modeled using MODELER (46). Residues 18–453 of the 587 residues (i.e., the N-terminal cytosolic domain) were modeled using the structure of the *S. cerevisiae* SAC1 (PDB ID code 1LWT, chain X), the closest homolog to human SAC1 with a known structure, as a template. The sequences of the human and yeast SAC1 are about 35% identical to one another. The models were evaluated using the statistical potentials of mean force and were found to have scores in the acceptable range of values. In all, five different models were built, but only one was chosen for further analysis as they varied by less than 0.5 Å in main-chain root mean-squared deviation from one another. Surface electrostatics were computed using the program APBS (47).

**ACKNOWLEDGMENTS.** We thank Dr. Blanche Schwappach (Göttingen University Medical School), Dr. Vivek Bhalla (Stanford University), and Dr. Gary Thomas (University of Pittsburgh) for kindly providing 14-3-3 constructs; Ann Fischer and Xiaozhu Zhang for providing tissue culture support; and Yusong Guo and David Melville for proof-reading the manuscript. This work was supported by grant from the Howard Hughes Medical Institute (HHMI) (to R.S.) and National Institutes of Health Grant R01 GM084088 (to P.M.). KBP is a past Human Frontiers Science Program postdoctoral long-term fellow and currently an HHMI research associate. M.S.M. would like to acknowledge a senior fellowship from the Wellcome Trust–Department of Biotechnology, India alliance. R.S. is a Senior fellow of the University of California, Berkeley Miller Institute.

- Barlowe C, et al. (1994) COPII: A membrane coat formed by Sec proteins that drive vesicle budding from the endoplasmic reticulum. *Cell* 77(6):895–907.
- Miller E, Antonny B, Hamamoto S, Schekman R (2002) Cargo selection into COPII vesicles is driven by the Sec24p subunit. *EMBO J* 21(22):6105–6113.
- Gillon AD, Latham CF, Miller EA (2012) Vesicle-mediated ER export of proteins and lipids. *Biochim Biophys Acta* 1821(8):1040–1049.
- Noda Y, Yoda K (2010) Sec26 facilitates endoplasmic reticulum to Golgi transport of a set of mannosyltransferases in *Saccharomyces cerevisiae*. *J Biol Chem* 285(20):15420–15429.
- Kurita T, Noda Y, Takagi T, Osumi M, Yoda K (2011) Kre6 protein essential for yeast cell wall beta-1,6-glucan synthesis accumulates at sites of polarized growth. *J Biol Chem* 286(9):7429–7438.
- Zanetti G, Pahuja KB, Studer S, Shim S, Schekman R (2012) COPII and the regulation of protein sorting in mammals. *Nat Cell Biol* 14(1):20–28.
- Espenshade PJ, Li WP, Yabe D (2002) Sterols block binding of COPII proteins to SCAP, thereby controlling SCAP sorting in ER. *Proc Natl Acad Sci USA* 99(18):11694–11699.
- Smith AJ, Daut J, Schwappach B (2011) Membrane proteins as 14-3-3 clients in functional regulation and intracellular transport. *Physiology (Bethesda)* 26(3):181–191.
- Bridges D, Moorhead GB (2005) 14-3-3 proteins: A number of functions for a numbered protein. *Sci STKE* 2005(296):re10.
- Fu H, Subramanian RR, Masters SC (2000) 14-3-3 proteins: Structure, function, and regulation. *Annu Rev Pharmacol Toxicol* 40:617–647.
- Ford JC, et al. (1994) 14-3-3 protein homologs required for the DNA damage checkpoint in fission yeast. *Science* 265(5171):533–535.
- Gelperin D, et al. (1995) 14-3-3 proteins: Potential roles in vesicular transport and Ras signaling in *Saccharomyces cerevisiae*. *Proc Natl Acad Sci USA* 92(25):11539–11543.
- Xing H, Zhang S, Weinheimer C, Kovacs A, Muslin AJ (2000) 14-3-3 proteins block apoptosis and differentially regulate MAPK cascades. *EMBO J* 19(3):349–358.
- Aitken A (1996) 14-3-3 and its possible role in co-ordinating multiple signalling pathways. *Trends Cell Biol* 6(9):341–347.
- van Heusden GP, et al. (1995) The 14-3-3 proteins encoded by the BMH1 and BMH2 genes are essential in the yeast *Saccharomyces cerevisiae* and can be replaced by a plant homologue. *Eur J Biochem* 229(1):45–53.
- Mrowiec T, Schwappach B (2006) 14-3-3 proteins in membrane protein transport. *Biol Chem* 387(9):1227–1236.
- Okamoto Y, Shikano S (2011) Phosphorylation-dependent C-terminal binding of 14-3-3 proteins promotes cell surface expression of HIV co-receptor GPR15. *J Biol Chem* 286(9):7171–7181.
- Rajan S, et al. (2002) Interaction with 14-3-3 proteins promotes functional expression of the potassium channels TASK-1 and TASK-3. *J Physiol* 545(Pt 1):13–26.
- Zuzarte M, et al. (2009) Intracellular traffic of the K<sup>+</sup> channels TASK-1 and TASK-3: Role of N- and C-terminal sorting signals and interaction with 14-3-3 proteins. *J Physiol* 587(Pt 5):929–952.
- Heusser K, et al. (2006) Scavenging of 14-3-3 proteins reveals their involvement in the cell-surface transport of ATP-sensitive K<sup>+</sup> channels. *J Cell Sci* 119(Pt 20):4353–4363.
- Yuan H, Michelsen K, Schwappach B (2003) 14-3-3 dimers probe the assembly status of multimeric membrane proteins. *Curr Biol* 13(8):638–646.
- Forrest S, et al. (2013) Increased levels of phosphoinositides cause neurodegeneration in a *Drosophila* model of amyotrophic lateral sclerosis. *Hum Mol Genet* 22(13):2689–2704.
- Blagoveshchenskaya A, et al. (2008) Integration of Golgi trafficking and growth factor signaling by the lipid phosphatase SAC1. *J Cell Biol* 180(4):803–812.
- Blagoveshchenskaya A, Mayinger P (2009) SAC1 lipid phosphatase and growth control of the secretory pathway. *Mol Biosyst* 5(1):36–42.
- Wang J, Chen J, Enns CA, Mayinger P (2013) The first transmembrane domain of lipid phosphatase SAC1 promotes Golgi localization. *PLoS ONE* 8(8):e71112.
- Konrad G, Schlecker T, Faulhammer F, Mayinger P (2002) Retention of the yeast Sac1p phosphatase in the endoplasmic reticulum causes distinct changes in cellular phosphoinositide levels and stimulates microsomal ATP transport. *J Biol Chem* 277(12):10547–10554.
- Faulhammer F, et al. (2007) Growth control of Golgi phosphoinositides by reciprocal localization of sac1 lipid phosphatase and pik1 4-kinase. *Traffic* 8(11):1554–1567.
- Piao H, Mayinger P (2012) Growth and metabolic control of lipid signalling at the Golgi. *Biochem Soc Trans* 40(1):205–209.
- Xue Y, et al. (2008) GPS 2.0, a tool to predict kinase-specific phosphorylation sites in hierarchy. *Mol Cell Proteomics* 7(9):1598–1608.
- Maehama T, Taylor GS, Slama JT, Dixon JE (2000) A sensitive assay for phosphoinositide phosphatases. *Anal Biochem* 279(2):248–250.
- Baker D, Sali A (2001) Protein structure prediction and structural genomics. *Science* 294(5540):93–96.
- Rittinger K, et al. (1999) Structural analysis of 14-3-3 phosphopeptide complexes identifies a dual role for the nuclear export signal of 14-3-3 in ligand binding. *Mol Cell* 4(2):153–166.
- Yaffe MB, et al. (1997) The structural basis for 14-3-3:phosphopeptide binding specificity. *Cell* 91(7):961–971.
- Aitken A (2002) Functional specificity in 14-3-3 isoform interactions through dimer formation and phosphorylation. Chromosome location of mammalian isoforms and variants. *Plant Mol Biol* 50(6):993–1010.
- Masters SC, Pederson KJ, Zhang L, Barbieri JT, Fu H (1999) Interaction of 14-3-3 with a nonphosphorylated protein ligand, exoenzyme S of *Pseudomonas aeruginosa*. *Biochemistry* 38(16):5216–5221.
- Petosa C, et al. (1998) 14-3-3zeta binds a phosphorylated Raf peptide and an unphosphorylated peptide via its conserved amphipathic groove. *J Biol Chem* 273(26):16305–16310.
- Henriksson ML, et al. (2002) A nonphosphorylated 14-3-3 binding motif on exoenzyme S that is functional in vivo. *Eur J Biochem* 269(20):4921–4929.
- Pozuelo Rubio M, et al. (2004) 14-3-3-affinity purification of over 200 human phosphoproteins reveals new links to regulation of cellular metabolism, proliferation and trafficking. *Biochem J* 379(Pt 2):395–408.
- Miller EA, et al. (2003) Multiple cargo binding sites on the COPII subunit Sec24p ensure capture of diverse membrane proteins into transport vesicles. *Cell* 114(4):497–509.
- Rohde HM, et al. (2003) The human phosphatidylinositol phosphatase SAC1 interacts with the coatamer I complex. *J Biol Chem* 278(52):52689–52699.
- Schindler AJ, Schekman R (2009) In vitro reconstitution of ER-stress induced ATF6 transport in COPII vesicles. *Proc Natl Acad Sci USA* 106(42):17775–17780.
- Kim J, Hamamoto S, Ravazzola M, Orzi L, Schekman R (2005) Uncoupled packaging of amyloid precursor protein and presenilin 1 into coat protein complex II vesicles. *J Biol Chem* 280(9):7758–7768.
- Fromme JC, et al. (2007) The genetic basis of a craniofacial disease provides insight into COPII coat assembly. *Dev Cell* 13(5):623–634.
- Merte J, et al. (2010) Sec24b selectively sorts Vangl2 to regulate planar cell polarity during neural tube closure. *Nat Cell Biol* 12(1):41–46; sup pp 41–48.
- Ohno H, et al. (1998) The medium subunits of adaptor complexes recognize distinct but overlapping sets of tyrosine-based sorting signals. *J Biol Chem* 273(40):25915–25921.
- Sali A, Blundell TL (1993) Comparative protein modelling by satisfaction of spatial restraints. *J Mol Biol* 234(3):779–815.
- Baker NA, Sept D, Joseph S, Holst MJ, McCammon JA (2001) Electrostatics of nanosystems: Application to microtubules and the ribosome. *Proc Natl Acad Sci USA* 98(18):10037–10041.